

Scientific paper  
UDC:620.193.197

A. S. FOUDA<sup>1</sup>, A. M. EL-DESOKY<sup>2</sup>,  
A. A. KESHK<sup>3</sup>

## Inhibitive effect of azine and diazine derivatives on the corrosion of 316L SS in acidic media

*The inhibiting effect of some azine and diazine derivatives on the corrosion of cyclic stressed 316L SS specimens in 3 M HCl in the presence of organic derivatives with concentrations ( $1 \times 10^{-6}$  M –  $11 \times 10^{-6}$  M) at 30°C was studied using weight loss and galvanostatic polarization techniques. The inhibition of these derivatives on the uniform corrosion was evaluated by anodic and cathodic polarization curves of the electrode in the tested media. The examined derivatives exerted an inhibiting action towards corrosion. Polarization studies revealed that these derivatives behave as mixed inhibitors and inhibit corrosion by parallel adsorption on the specimen surface due to the presence of more than one active centre in the inhibitor molecule. The adsorption obeyed Temkin adsorption isotherm. The inhibitor efficiency increases with increasing the concentration of the inhibitor and decreases with increasing the value of the cyclic stress. Addition of  $I^-$ ,  $Br^-$  and  $SCN^-$  ions to the solution containing organic derivatives increases the inhibition efficiency of the system.*

**Keywords:** Organic derivatives; Inhibition; Cyclic stress; Acidic media; 316L SS.

321 stainless steel was attributed to the effect of retarding both anodic and cathodic reactions of the corrosion processes [5]. SCC of AISI 321 stainless steel in acidic solution was inhibited by thiourea and its derivatives, primary amines and tetra-amine salts and estimating the anodic and cathodic action coefficients of the corrosion process, it was found that those inhibitors reduced the rate of anodic dissolution of the steel [6,7].

The previous studies were mostly performed by SSRT combined with observation of the morphology of fractured specimens and electrochemical measurements of unstressed specimens. It is expected that in situ electrochemical measurements of the corrosion rate of stressed specimens under dynamic straining condition may offer some interesting information on the role of an inhibitor.

In this paper, the inhibition effect of organic derivatives on the corrosion fatigue (CF) of 316L SS specimens stressed by cyclic stress with cyclic frequency of 10.5 Hz while immersed in hydrochloric acid solution is assessed by using in situ measurements of electrochemical galvanostatic polarization.

### EXPERIMENTAL DETAIL .2

#### Materials and solution .2.1

The chemical composition and mechanical properties of specimen material are given in Tables 1 and 2).

### INTRODUCTION .1

Stress corrosion cracking (SCC) is one of the most serious corrosion problems facing metallic materials during their service life. Much attention has been paid to avoid or eliminate the damage of metallic materials due to SCC especially when there is a cyclic stress on the metallic material. SCC is sensitive to the composition of the corrosion environment; the addition of small amount of proper inhibitor mitigated SCC of austenitic steels in acidic media [1].

Benzotriazole (BTA) decreased the susceptibility of SCC for 18Cr-9Ni-Ti stainless steel in acidic chloride solution [1]. Inhibitors such as phenylthiourea, benzotriazole and acridine significant influence in the case of SCC tests with constant load than in constant strain rate testing (CSRT) [2]. Other inhibitors such as benzimidazole-2-thiol, benzothiazole-2-thiol, phenylthiourea and a mixture of n-decylamine + KI were found to be effective in the case of SCC tests by slow strain rate (SSRT) and U-bend [3,4].

The synergistic inhibition effect of iodine ions with some amines in NaCl solution on SCC of AISI

---

Author's address: <sup>1</sup>Department of Chemistry, Faculty of Science, El-Mansoura University, El-Mansoura-35516, Egypt, <sup>2</sup>Chemistry Department, High Institute of Engineering & Technology (New Damietta), Egypt, <sup>3</sup>Department of Chemistry, Faculty of Science, University of Tabuk, Tabuk, Saudi Arabia

Received for Publication: 17. 07. 2014.

Accepted for Publication: 14. 09. 2014.

Table 1 - Chemical composition (wt %) of the 316L SS

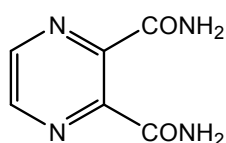
Material Type	Percent composition								
	C	Mn	P	S	Si	Cr	Ni	Mo	Cu
316L SS	0.02	1.0	0.054	0.02	1.0	16	11	3	0.2

Table 2 - The mechanical properties of 316L SS

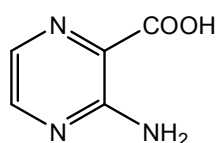
Yield stress (Mpa)	Tensile strength (Mpa)	Elongation (Lo=5do)%
335	322	19

HCl, KSCN, KI, KBr and organic permidine derivatives all of BDH made were used for preparing solutions. The names and molecular structures of the derivatives are given in bellow:

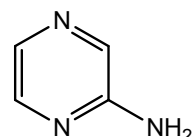
## Series 1



pyrazine-2,3-dicarboxamide

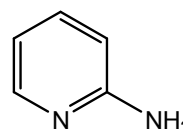


3-aminopyrazine-2-carboxylic acid

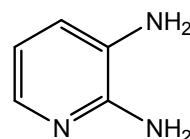


pyrazin-2-amine

## Series 2



pyridin-2-amine



pyridine-2,3-diamine

Series 1: (I) > (II) > (III)

Series 2: (IV) > (V)

solution, rinsed with double distilled water, dried as before and weighed again. The average weight loss at a certain time for each set of three samples was taken. The weight loss was recorded to the nearest 0.0001g.

Electrochemical technique (Galvanostatic -2.2.2 polarization method)

## a. Electrodes

Chemical composition of 316L SS used in this study is given in Table 1. Two different types of electrodes were used; disks with 12 mm diameter and 2 mm thickness and cylindrical specimens. The discs were welded from one side to a copper wire for electric connection and embedded in glass tube of larger diameter than the sample. Epoxy

## Experimental .2.2

## Chemical Technique (Weight loss method) .2.2.1

The reaction basin was graduated glass vessel 6 cm inner diameter and having a total volume of 250 ml. 100 ml of the test solution were employed in each experiment. The test pieces were cut into 2×2×0.2 cm. They were mechanically polished with emery paper (a coarse paper was used initially and then progressively finer grades were employed), rinsed with double distilled water and finally dried between two filter papers and weighed. The test pieces were suspended by suitable glass hooks at the edge of the basin, and under the surface of the test solution by about 1cm. After specified periods of time, 3 test pieces were taken out of the test

mm while the gage length of the middle part was 20 mm and its diameter was 4 mm, and the overall length was 140 mm as shown in Figure 1. The gage length of all specimens were prepared by treatment with emery papers n. 1000, then degreased in acetone ultrasonic bath, washed with bi-distilled water and dried.

resin was used to stick the sample to the glass tube except the exposed tested surface area which was left to be exposed to the corrosive media.

Cylindrical specimens were used in the fatigue test and in electrochemical measurements after fatigue test in air. The specimen diameter was 10

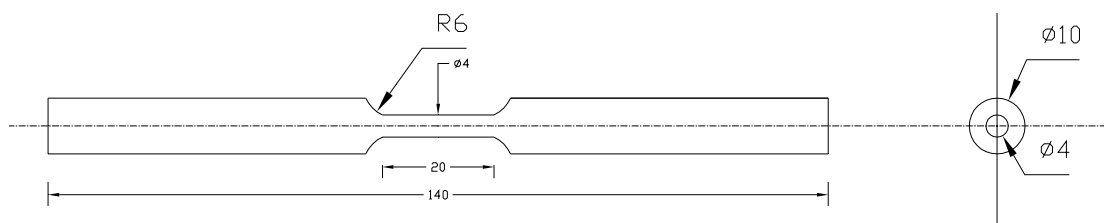


Figure 1 - Specimen of fatigue test (Dim. mm)

Concentration M	Inhibition %				
	(I)	(II)	(III)	(IV)	(V)
$10^{-6} \times 1$	78.2	70.2	65.0	57.2	54.2
$10^{-6} \times 3$	81.3	73.3	68.0	61.1	57.1
$10^{-6} \times 5$	83.7	76.2	71.2	64.3	59.1
$10^{-6} \times 7$	86.1	79.2	74.3	68.1	62.0
$10^{-6} \times 9$	89.0	82.1	78.5	72.0	65.1
$10^{-6} \times 11$	91.0	85.3	80.4	74.3	67.2

It can be seen from Table 4 that the addition  $10^{-2}$  M of KI, and inhibits the corrosion of 316L SS to a large extent and by increasing the concentration of hydrazide derivatives ( $1 \times 10^{-6}$  -  $11 \times 10^{-6}$  M) the percentage inhibition increases. This can be interpreted according to Schmitt and Bedbur [8], which proposed two types of joint adsorption namely competitive and cooperative. In competitive adsorption, the anions and cations are adsorbed at different sites on the electrode surface, and in case of cooperative adsorption, the anions are chemisorbed on the electrode surface and the cations are adsorbed on a layer of the anion, apart from the adsorption on the surface directly.

From the data of Table 4 it is seen that KI would be considered as one of the effective anions for synergistic action with respect to the investigated salts. The net increment of inhibition efficiency shows a synergistic effect of KI, KSCN and KBr with hydrazide derivatives. The synergistic effect depends on the type and concentration of anions. The inhibition efficiency in presence of these anions decreases in the order: KI > KSCN > KBr [9]. The experimental results suggested that the presence of these anions in the solution stabilizes the adsorption of derivatives on the metal surface and improved the inhibition efficiency of these derivatives.

The figure 3 demonstrates the mass- loss time curves for the dissolution of 316L SS in 3 M HCl in absence and presence of different concentrations of compound (b) without and with addition of  $10^{-2}$  M KI at 30°C.

$$S_{\theta} = (1 - \theta_{1+2}) / (1 - \theta'_{1+2}) \quad (3)$$

$$\text{where } \theta_{1+2} = \theta_1 + \theta_2 - \theta_1 \theta_2$$

$\theta'_{1+2}$  - measured surface coverage by the anion in combination with cation.  $\theta_1$  and  $\theta_2$  are the surface coverage for anions and cations, respectively.

Table 5 lists the variation of the synergistic parameter ( $S_{\theta}$ ) in the presence of different concentrations of derivatives. It is seen that all values of ( $S_{\theta}$ ) are less than unity and, therefore, the adsorption of each compound antagonizes the other's adsorption. Thus, derivatives significantly

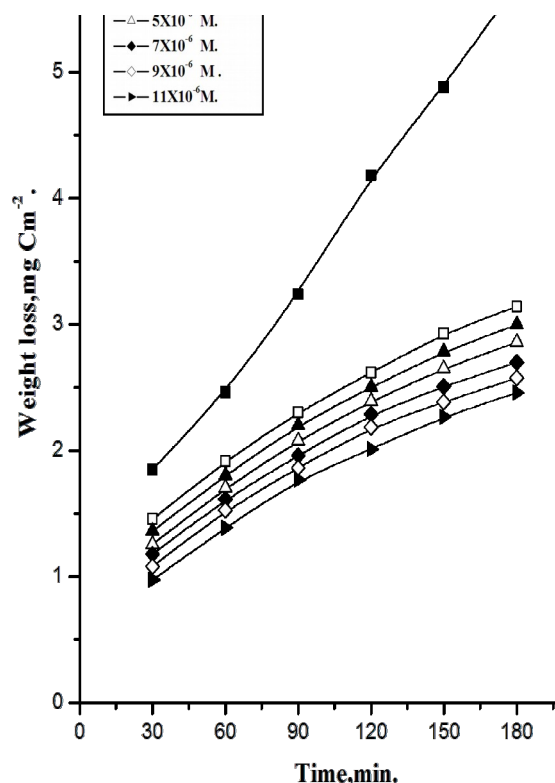


Figure 2 – Weight loss-time curves for the dissolution of 316 SS in 3 M HCl at 30°C

Figure 2 – Weight loss-time curves for the dissolution of 316 SS in absence and presence of different concentrations of compound (I) at 30°C

Table 3 - % Inhibition of 316L SS dissolution at 120 min. immersion in 3 M HCl in presence of different concentrations of inhibitors at 30°C

Concentration, M	Inhibition %				
	(I)	(II)	(III)	(IV)	(V)
$10^{-6} \times 1$	68.4	61.3	56.7	44.3	37.1
$10^{-6} \times 3$	71.5	65.7	59.3	47.7	40.5
$10^{-6} \times 5$	74.1	68.1	63.6	50.0	42.3
$10^{-6} \times 7$	77.0	71.2	65.4	53.1	45.2
$10^{-6} \times 9$	78.3	74.1	67.2	55.3	47.1
$10^{-6} \times 11$	81.2	77.3	70.8	59.1	51.2

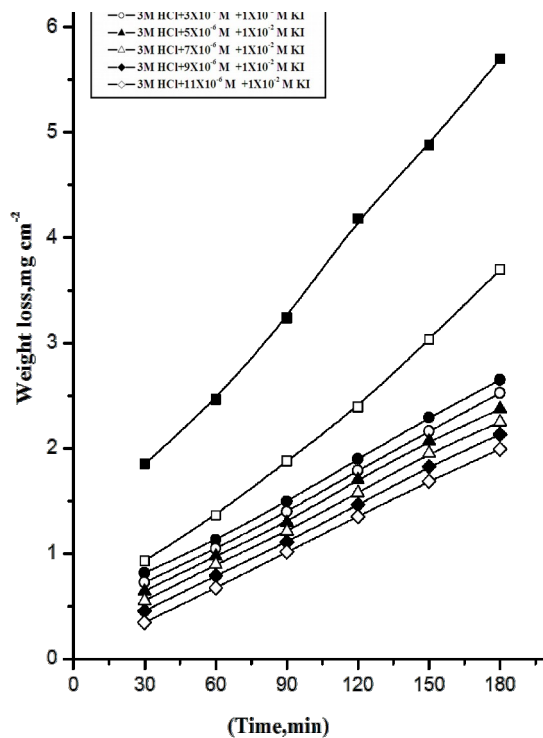
### Synergistic effect .3.2

As seen from Table 3, the percentage inhibition efficiency of the tested derivatives is low, so in order to increase these values we use KI, KSCN, and KBr in addition to the different concentrations of the investigated derivatives. Table 4 shows the % In. of the investigated derivatives in presence of  $1 \times 10^{-2}$  M of KI.

Table 4 - % Inhibition efficiency of 316L SS dissolution at 120 min. immersion in 3M HCl in presence of  $1 \times 10^{-2}$  M KI at different concentrations of inhibitors at 30°C

Figure 3 - Weight loss-time curves for 316 SS dissolution 3M HCl in absence and presence of  $1 \times 10^{-2}$  M KI and different concentrations of inhibitor (I) at  $30^\circ\text{C}$

improved the coverage and thus the quality and inhibition efficiency of derivatives on the corroding 316L SS.



Weight loss-time curves for 316L SS dissolution in 3M HCl in

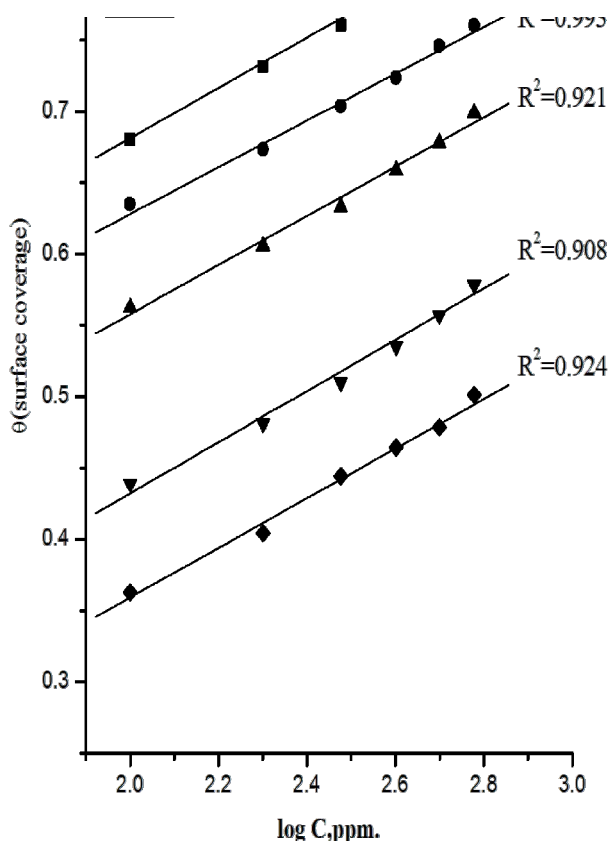


Figure 5 – Curve fitting of corrosion data for 316L SS HCl in presence of different concentrations of inhibitors to the Temkin isotherm at 30 °C

#### Effect of Temperature .3.4

The effect of temperature (30 – 55°C) on the performance of the inhibitors at a concentration of ( $1 \times 10^{-6}$  -  $11 \times 10^{-6}$  M) for 316L SS in 3M HCl was studied using Weight-loss measurements. Plots of  $\log k$  (corrosion rate) against  $1/T$  (absolute temperature) Figure 6 for 316L SS in 3M M HCl, gave straight lines. The values of the slopes obtained at different temperatures permit the calculation of Arrhenius activation energy ( $E_a$ ). The activation energy values obtained from these lines were found to be 58 kJ mol<sup>-1</sup> for 316L SS 3M HCl and 3 kJ mol<sup>-1</sup> for acid containing inhibitors 3, Table 7.

Table 7 - Effect of concentrations of inhibitors on the activation energy of 316L SS dissolution in 3M HCl

Concentration, M	Activation energy, $E_a$ , kJ mol <sup>-1</sup>				
	(I)	(II)	(III)	(IV)	(V)
0.0	58.0				
$10^{-6} \times 1$	90.0	80.7	67.8	61.4	61.0
$10^{-6} \times 3$	94.4	81.0	74.1	70.2	64.5
$10^{-6} \times 5$	96.4	83.2	75.2	70.9	64.9
$10^{-6} \times 7$	96.6	84.0	76.8	71.9	65.0
$10^{-6} \times 9$	97.3	85.0	78.2	72.9	65.1
$10^{-6} \times 11$	97.	86.	80.	73.	66.

active sites occupied by one hydrazide molecule and  $C$  is the bulk concentration of the inhibitor. From Table 6 it is noted that  $\Delta G_{ads}$  values have a negative sign indicating that the adsorption process proceeds spontaneously and increase as the percentage inhibition increases. Table 6 shows the calculated thermodynamic parameters.

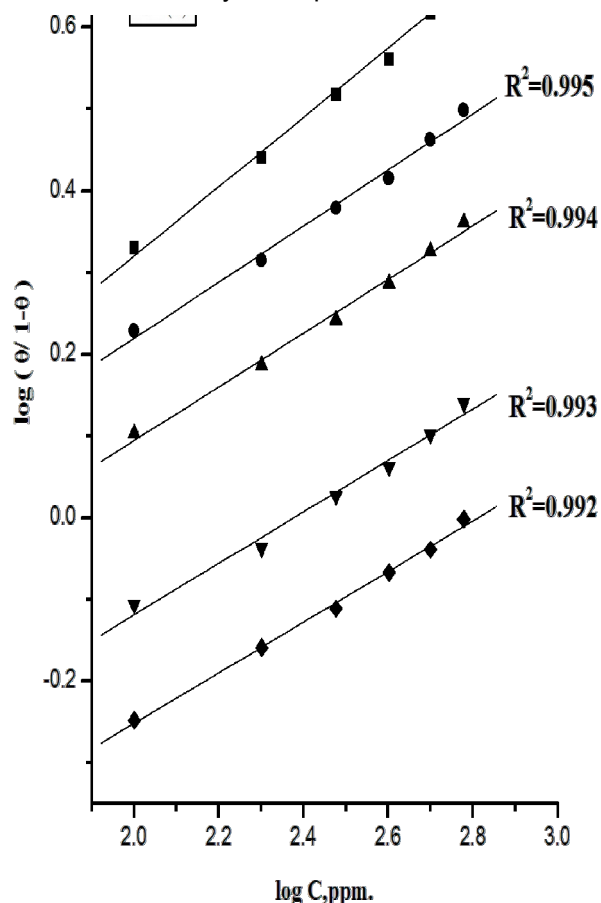


Figure 4 - Curve fitting of corrosion data for 316L SS in 3M HCl in presence of inhibitors (I) to the kinetic model at 30 °C

Table 6 - Inhibitor binding constant ( $K$ ), free energy of binding ( $\Delta G_{ads}$ ), number of active sites ( $1/y$ ) and later interaction parameter ( $a$ ) for inhibitors derivatives at 30°C

Inhibitors	Kinetic model			Temkin		
	$y/1$	$K$	$\Delta G_{ads}$ , kJmol <sup>-1</sup>	$a$	$K$	$\Delta G_{ads}$ , kJmol <sup>-1</sup>
(I)	3.200	0.985	60.7	14.03	72.3	63.0
(II)	3.121	0.874	58.9	13.33	67.1	62.2
(III)	3.023	0.655	54.5	13.24	17.1	52.1
(IV)	2.897	0.572	52.4	12.99	2.53	37.5
(V)	2.313	0.435	48.27	12.82	1.16	31.6

Figure 7 –  $\log k - 1/T$  curves for 316L SS dissolution in 3M HCl in absence and presence of different concentrations of inhibitor (I)

Activation parameters for corrosion of zinc were calculated from Arrhenius – type plot.

$$k = A \exp(-E_a^* / RT) \quad (6)$$

and transition state- type equation :

$$k = RT / Nh \exp(\Delta S^* / R) \exp(-\Delta H^* / RT) \quad (7)$$

The relation between  $\log k/T$  vs.  $1/T$  gives straight line, from its slope,  $\Delta H^*$  can be computed and from its intercept  $\Delta S^*$  can be also computed Figure 7.

Tables 8 and 9 exhibits the values of apparent activation energy  $E_a^*$ , enthalpies  $\Delta H^*$  and entropies  $\Delta S^*$  for 316L SS in dissolution in 3M HCl solution. The presence of derivatives increases the activation energies of 316L SS indicating strong adsorption of the inhibitor molecules on the metal surface and the presence of these additives induces energy barrier for the corrosion reaction and this barrier increases with increasing the additive concentrations.

Table 8 - Effect of concentrations of inhibitors on the activation enthalpy of 316L SS dissolution in 3M HCl

Concentration M	Activation enthalpy, $\Delta H^*$ , kJ mol <sup>-1</sup>				
	(I)	(II)	(III)	(IV)	(V)
0.0	52.6				
$10^{-6} \times 1$	87.4	76.8	71.4	67.0	62.0
$10^{-6} \times 3$	89.5	78.7	71.9	67.1	62.2
$10^{-6} \times 5$	92.2	80.6	74.1	68.2	63.2
$10^{-6} \times 7$	92.6	81.3	75.5	69.2	63.3
$10^{-6} \times 9$	94.3	82.7	79.4	69.9	64.8
$10^{-6} \times 11$	94.3	83.4	80.2	70.2	65.1

Table 9 - Effect of concentrations of inhibitors on the activation entropy of 316L SS dissolution in 3M HCl

Concentration, M	Activation entropy, $-\Delta S^*$ , k <sup>-1</sup> J mol <sup>-1</sup>				
	(I)	(II)	(III)	(IV)	(V)
0.0	82.8				
$10^{-6} \times 1$	7.3	25.0	41.0	54.5	70.0
$10^{-6} \times 3$	13.4	19.7	36.9	53.3	69.5
$10^{-6} \times 5$	20.9	14.4	33.5	51.6	69.0
$10^{-6} \times 7$	21.7	12.7	29.5	48.9	66.7
$10^{-6} \times 9$	26.0	8.8	17.4	47.3	66.0
$10^{-6} \times 11$	26.7	7.4	13.4	46.4	65.2

### Electrochemical measurement 3.5

Galvanostatic polarization studies were carried out on 316LL SS in 3 M HCl solution without and

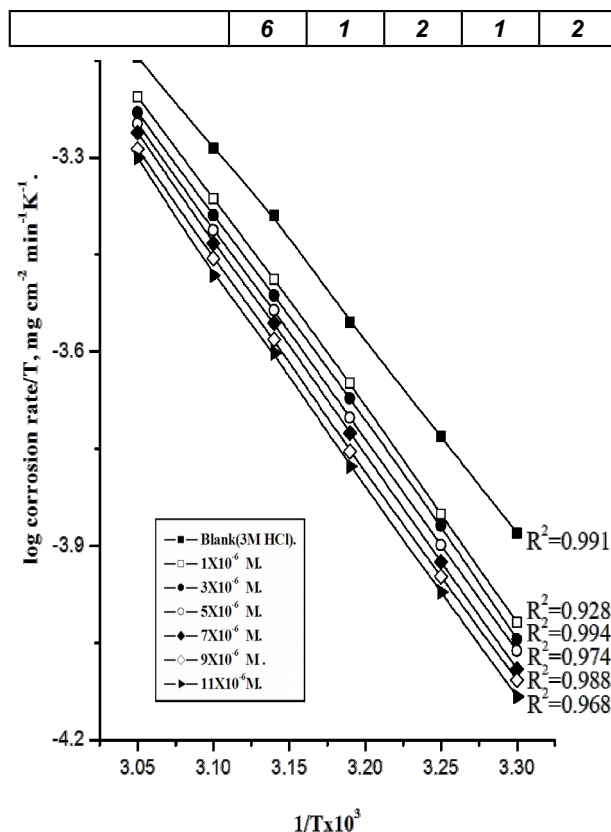


Figure 6 -  $\log (\text{corrosion rate}/T) - (1/T)$  curves for 316L SS dissolution in 3M HCl in absence and presence of different concentrations of inhibitor (I)

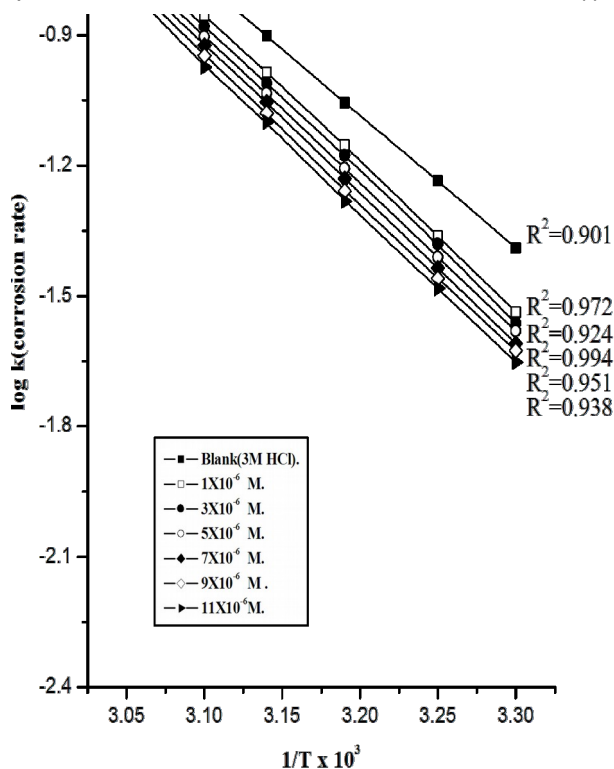


Figure 8 – Galvanostatic polarization curve of 316L SS in absence and presence of different concentration of inhibitor (I) at 30 °C

Tafel slopes ( $\beta_a$  &  $\beta_c$ ) values, corrosion potential ( $E_{corr}$ ), corrosion current ( $i_{corr}$ ), degree of surface coverage ( $\theta$ ) and inhibition efficiency (% IE) indicate that:

1- The corrosion current density decreases with increasing the concentration of organic derivatives. This indicates that the presence of these derivatives retards the dissolution of 316LL SS in 3M HCl solution and the degree of inhibition depends on the concentration and type of the inhibitor present as shown in Figure 8.

2 - The degree of surface coverage was found to increase with increasing the concentration of inhibitor.

3 - The presence of the tested inhibitors retards both anodic and cathodic reactions and hence these inhibitors act as mixed type inhibitors.

4 - The order of decrease in inhibition efficiency for the tested additives is:

Series 1: (I) > (II) > (III)

Series 2: (IV) > (V)

with different concentrations of the inhibitors. The tested specimen was used as working electrode. Saturated calomel electrode (SCE) was used as reference electrode while platinum wire as a counter electrode. All experiments were carried out at 30°C. The inhibition efficiency (%IE) is defined as [10]:

$$\%IE = ((i_{corr.} - i_{inh.}) / i_{corr.}) \times 100 \quad (8)$$

Where  $i_{corr.}$  and  $i_{inh.}$  are the corrosion current density in the absence and presence of inhibitors respectively. The degree of surface area coverage ( $\theta$ ) can be calculated from the relation:

$$\theta = (i_{corr.} - i_{inh.}) / i_{corr.} \quad (9)$$

### Polarization curves .3.5.1

Corrosion behavior of 316LL SS is studied in 3M HCl solutions in absence and presence of ( $1 \times 10^{-6}$  –  $11 \times 10^{-6}$ ) M inhibitors (I –V) at 30°C. Figure 7 show the galvanostatic polarization curve of 316LL SS in 3M HCl in absence and presence of inhibitor (I) at different inhibitor concentrations, Table (10) gives the various corrosion parameters.

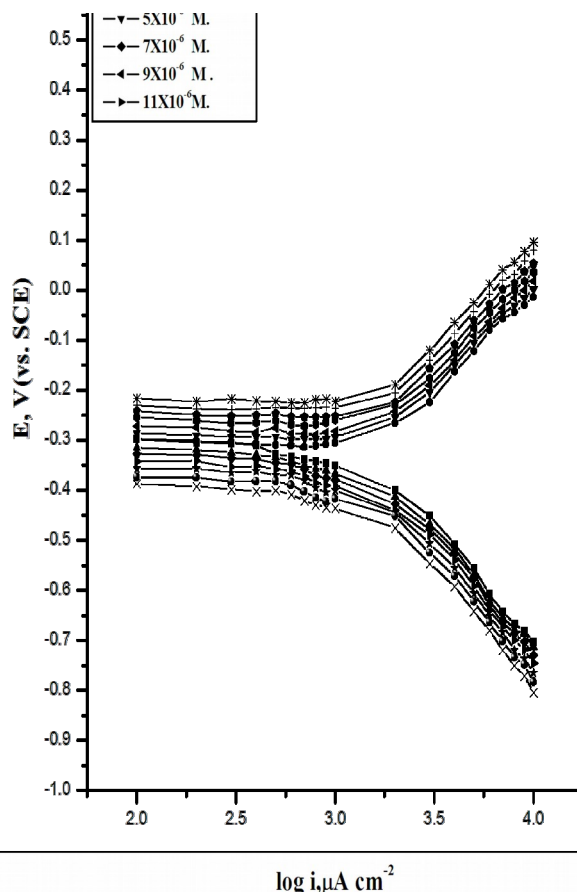


Fig (7) -Galvanostatic polarization curve of 316L SS in 3M HCl in the presence of different concentrations of inhibitor (I–V) at 30°C

Table 10 - corrosion parameters for 316L ss in 3M HCl in absence and presence of different concentrations of inhibitors (I–V) at 30°C

Inhibitor	Conc., M	-E <sub>cor</sub>	i <sub>cor</sub> , μAcm <sup>-2</sup>	B <sub>a</sub> , mVdec <sup>-1</sup>	B <sub>c</sub> , mVdec <sup>-1</sup>	θ	%IE
-----------	----------	-------------------	---------------------------------------	--------------------------------------	--------------------------------------	---	-----



		V					
Blank	3M HCl	0.351	74.64	0.287	0.179	–	–
I	$1 \times 10^{-6}$	0.317	54.81	0.109	0.462	0.3862	38.62
	$3 \times 10^{-6}$	0.313	21.88	0.103	0.403	0.6143	61.43
	$5 \times 10^{-6}$	0.303	20.79	0.162	0.351	0.7443	74.43
	$7 \times 10^{-6}$	0.301	11.48	0.153	0.362	0.8462	84.62
	$9 \times 10^{-6}$	0.297	11.21	0.148	0.298	0.8498	84.98
	$11 \times 10^{-6}$	0.287	10.93	0.158	0.197	0.8535	85.35
II	$1 \times 10^{-6}$	0.330	50.70	0.052	0.192	0.3208	32.08
	$3 \times 10^{-6}$	0.319	32.81	0.056	0.243	0.5605	56.06
	$5 \times 10^{-6}$	0.315	17.10	0.088	0.218	0.7709	77.09
	$7 \times 10^{-6}$	0.306	13.68	0.113	0.207	0.8169	81.69
	$9 \times 10^{-6}$	0.301	12.91	0.111	0.312	0.8270	82.70
	$11 \times 10^{-6}$	0.297	11.56	0.103	0.301	0.8451	84.51
III	$1 \times 10^{-6}$	0.333	51.40	0.051	0.190	0.2940	29.40
	$3 \times 10^{-6}$	0.331	36.30	0.061	0.208	0.5355	53.55
	$5 \times 10^{-6}$	0.327	28.18	0.083	0.206	0.6656	66.56
	$7 \times 10^{-6}$	0.316L	14.36	0.069	0.347	0.7672	76.72
	$9 \times 10^{-6}$	0.312	15.83	0.110	0.351	0.7879	78.79
	$11 \times 10^{-6}$	0.297	14.96	0.097	0.309	0.7995	79.95
IV	$1 \times 10^{-6}$	0.339	57.81	0.063	0.425	0.2255	22.55
	$3 \times 10^{-6}$	0.333	36.31	0.077	0.392	0.4962	49.62
	$5 \times 10^{-6}$	0.326	29.38	0.084	0.391	0.6295	62.95
	$7 \times 10^{-6}$	0.323	18.71	0.114	0.386	0.7407	74.07
	$9 \times 10^{-6}$	0.316L	17.96	0.127	0.389	0.7593	75.93
	$11 \times 10^{-6}$	0.302	15.32	0.132	0.371	0.7947	79.47
V	$1 \times 10^{-6}$	0.341	59.71	0.064	0.427	0.2000	20
	$3 \times 10^{-6}$	0.336	40.38	0.089	0.393	0.4590	45.90
	$5 \times 10^{-6}$	0.325	30.42	0.093	0.390	0.5924	59.24
	$7 \times 10^{-6}$	0.321	21.21	0.128	0.372	0.7158	71.58
	$9 \times 10^{-6}$	0.302	18.51	0.136	0.363	0.7520	75.20
	$11 \times 10^{-6}$	0.292	16.21	0.148	0.348	0.7828	78.28

inhibitor has less adsorption affinity on them. When the adsorption density reaches monolayer adsorption Figure 9b, some of the nucleation sites begin to be completely covered by inhibitor molecules. At maximum adsorption density in Figure 9c, the whole surface, including the nucleation sites, is covered by the inhibitor molecules and hence complete inhibition occurs.

The inhibition mechanism of the tested inhibitor is a combination of surface blockage and electrostatic repulsion between adsorbed surfactant layer and chloride ions. The adsorption density of inhibitor depends on the inhibitor concentration. At adsorption density less than that needed for monolayer coverage Figure 9a, most of the nucleation sites are still possibly exposed to HCl, as the inhi-

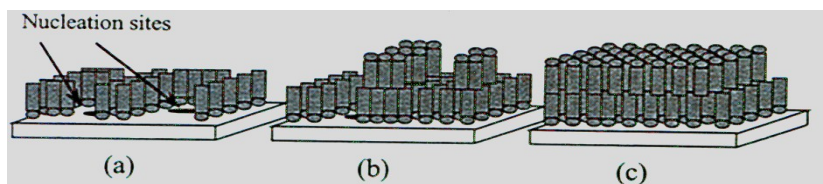


Figure 9 - Adsorption schemes for organic compound as an inhibitor on 316L SS stainless steel, (8a) at low concentrations, (8b) intermediate concentrations and (8c) high concentrations

atoms in less strained sites. Consequently, corrosion of the most strained regions of a metal have the highest rate of corrosion.

The polarization curves were plotted for each inhibitor as shown in Figure 10. The results indicate that, the inhibition efficiency of inhibitors (I–V) for the corrosion of 316L SS in the acidic solution at 30°C is decreased in order Series 1: (I) > (II) > (III) and Series 2: (IV) > (V) with increasing the concentration of inhibitors and decreased with increasing applied cyclic stresses as shown in Table 11. The corrosion of the most strained regions of the tested specimens is most rapid, also the adsorbed layer of inhibitor on stainless steel surface becomes less stable and the corrosive media becomes more aggressive. Inspection of Tafel slopes values and  $E_{\text{corr}}$  values under these conditions indicate that these inhibitors act as mixed – type inhibitors. Also, the corrosion current density  $i_{\text{corr}}$  increased with increasing the applied cyclic stresses. The increase in the applied cyclic stress adds to the free energy of the strained atoms and hence more atoms go to the solution causing a pronounced increase in the corrosion current density.

### Effect of applied cyclic stresses on the corrosion behavior of stainless steel 304 SS

In these experiments the measurements were carried out in 3 M HCl solution at 30°C in absence and presence of different inhibitors at different concentrations ( $5 \times 10^{-6}$  M –  $11 \times 10^{-6}$  M), while applying cyclic stresses (82Mpa - 247Mpa) with number of cycles (63000) at 10.5 Hz. The galvanostatic polarization curves were plotted for each inhibitor. In the rotating cantilever bending fatigue test, the tension and compression cyclic stresses occur at the outer surfaces of the specimen, for this reason plastic deformation commonly occurs by the slip of one plane over the other. Such slip is very non-uniform within a polycrystalline solid and can occur on only some of the crystal planes within a metal grain [11]. Stressed 316L SS surfaces by the rotating cantilever bending fatigue test, contain iron atoms that are more reactive hence they have a less stable crystalline environment and more susceptible to attack. Whenever a metal is stressed, the metallic crystal lattice becomes severely strained and tends to become more anodic, hence they travel into solution more readily than the

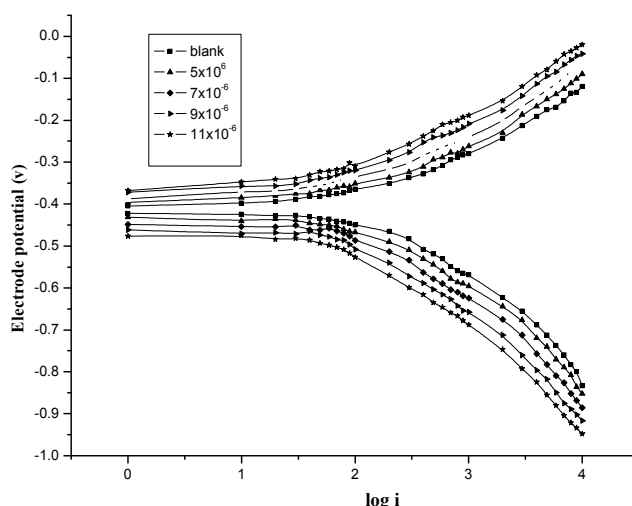


Fig.(9) Galvanostatic polarization curves of 316L SS in 3M HCl in absence and presence of inhibitor (I) at various concentrations at 30°C.

Figure 10 – Galvanostatic polarization curves of 316L SS in 3M HCl in absence and presence of inhibitor (I) at various concentrations at 30 °C

Table 11 - Corrosion parameters for 316L SS in 3M HCl in absence and presence of different concentrations of inhibitors (I–V) for stressed specimen by 247 MPa, at 63000 cycles at 30°C

Inhibitor	Conc., M	$-E_{\text{corr}}$ , V	$i_{\text{corr}}$ , $\mu\text{Acm}^{-2}$	$B_a$ , $\text{mVdec}^{-1}$	$B_c$ , $\text{mVdec}^{-1}$	$\theta$	%IE
Blank	2M HCl	0.391	141.25	0.280	0.325	–	–
I	$5 \times 10^{-6}$	0.382	107.15	0.197	0.352	0.2414	24.14
	$7 \times 10^{-6}$	0.381	102.80	0.211	0.399	0.2722	27.22
	$9 \times 10^{-6}$	0.376	79.72	0.161	0.347	0.3081	30.81
	$11 \times 10^{-6}$	0.372	93.32	0.173	0.325	0.3393	33.93
II	$5 \times 10^{-6}$	0.381	109.64	0.140	0.338	0.2237	22.37

	$7 \times 10^{-6}$	0.380	107.15	0.162	0.325	0.2414	24.14
	$9 \times 10^{-6}$	0.379	105.19	0.137	0.317	0.2552	25.52
	$11 \times 10^{-6}$	0.374	102.32	0.158	0.330	0.2586	25.86
III	$5 \times 10^{-6}$	0.369	118.85	0.279	0.431	0.1586	15.86
	$7 \times 10^{-6}$	0.367	117.76	0.293	0.407	0.1663	16.63
	$9 \times 10^{-6}$	0.361	106.69	0.272	0.398	0.2446	24.46
	$11 \times 10^{-6}$	0.349	106.32	0.235	0.379	0.2472	14.72
IV	$5 \times 10^{-6}$	0.366	128.23	0.307	0.396	0.92	9.2
	$7 \times 10^{-6}$	0.355	125.89	0.310	0.413	0.1087	10.87
	$9 \times 10^{-6}$	0.360	110.42	0.417	0.462	0.2182	21.82
	$11 \times 10^{-6}$	0.362	108.65	0.299	0.397	0.2307	23.07
V	$5 \times 10^{-6}$	0.361	131.25	0.306	0.382	0.0707	7.07
	$7 \times 10^{-6}$	0.357	128.74	0.312	0.405	0.0885	8.85
	$9 \times 10^{-6}$	0.361	123.66	0.423	0.446	0.1245	12.45
	$11 \times 10^{-6}$	0.364	122.64	0.405	0.376	0.1317	13.17

acidic chloride solution" *Corros. Sci.*, no 40(7), pp. 1109-1117.

- [2] D.E.Davies, J.P.Dennison, A.A.Odeh (1985), Proceedings of 6th European Symposium on Corrosion Inhibitors (6th. SEIC), ANN. Univ. Ferrara, N.S. Sez. V. Suppl. no. 8, pp. 669.
- [3] A.Frignani, G.Trabanelli, F.Zucchi (1984), "the use of slow strain rate technique for studying stress corrosion cracking inhibition" *Corros. Sci.*, no 24, pp.917-927
- [4] F.Zucchi, G.Trabanelli, A. Frignani, V.Carassiti, (1973), *5eme Congress European de Corrosion*, Paris, 24-28 September, pp. 217.
- [5] X. Z.Chen, S.H. Wu (1985), Proceedings of the 6th European Symposium on Corrosion Inhibitors (6th. SEIC), ANN. Univ. Ferrara, N.S. Sez. V. Suppl. no. 8, pp 677.
- [6] C.N.Cao, Q.G.Yang, M.Lu, H.C.Lin (1992), "you liang de nai shi cai liao hua gang yan zhe jiang sheng dong tou xian hua gang yan kai cai zong chang cai fang ce ji" *J. Chinese Soc. Corros. Protection*, no.2, pp.109-115
- [7] C. N. Cao, Corrosion Science and protection Technique (1990), no.2, pp. 1
- [8] G.Schmitt, K.Bedbur (1985) "Investigations on structural and electronic effects in acid inhibitors by AC impedance", *Werkst. Ü.Korros*, no. 36, pp. 273-278
- [9] E. Khamis, E.S.H. El- Ashry, A.K. Ibrahim (2000), "Synergistic action of vinyl triphenyl phosphonium bromide with various anions on corrosion of steel" *Br. Corros.J.*, no35 (2), pp.150-154
- [10] Y.A.El- Awady, A.I. Ahmed (1985), "Effect of temperature and inhibitors on the corrosion of aluminum in 2N HCl solution, A kinetic study" *J. Ind. Chen.*, no.24, pp.601-617
- [11] E. Dieter George, Mechanical Metallurgy, University of Maryland, (1988).

## CONCLUSIONS .4

The following conclusions can be deduced from the present study:

1- Derivatives appear to be efficient inhibitors for corrosion of 316L in 3MHCl solution, which act as mixed type inhibitors, the %IE was found to increase by increasing the inhibitor concentration and was found inhibitor (I) with high molecular weight which gives the highest inhibition efficiency over the other derivatives Series 1: (I) > (II) > (III) and Series 2: (IV) > (V).

2 - The inhibition of corrosion of 316LL SS in 3M HCl solution was found to obey the Temkin adsorption isotherm and the inhibitors appear to add to the passive layer formed on the tested 316L SS.

3 - Derivatives can be used as inhibitors to fatigue corrosion of 316L SS in HCl solution and these materials act as a mixed type inhibitors.

4 -The inhibition efficiency (%IE) increases with the increase in the inhibitor concentration, while decreases with the increase in the cyclic stress and the order of intensity of inhibition efficiency of inhibitors used was Series 1: (I) > (II) > (III) and Series 2: (IV) > (V).

5 -The corrosion current density increases with the increase in the cyclic stresses.

## REFERENCES

- [1] L. Niu, C.N. Cao, H.C. Lin, G.L. Song (1998), "Inhibitive effect of benzotriazole on the stress corrosion cracking of 18cr-9ni-ti stainless steel in

## IZVOD

### UTICAJ INHIBITORA DERIVATA AZINA I DIAZINA NA KOROZIJU NERĐAJUĆEG ČELIKA 316 LSS U KISELOJ SREDINI

*Inhibitorski efekat nekih derivata azina i diazina na koroziju 316L SS uzoraka u 3 M HCl u prisustvu organskih derivata sa koncentracijama ( $1 \times 10^{-6}$  M -  $11 \times 10^{-6}$  M) na 30°C je ispitivan preko gubitka težine i tehnikom galvanske polarizacije. Inhibitorski efekat ovih derivata na ravnomernost korozije uzoraka je ocenjivan preko anodnih i katodnih polarizacionih krivih elektrode u testiranim medijima. Ispitivani derivati vršili su inhibiciju korozije ispitivanih uzoraka. Polarizaciona ispitivanja su pokazala da se ovi derivati ponašaju kao mešani inhibitori i inhibiraju koroziju adsorpcijom čestica inhibitora na površini uzorka zbog prisustva više od jednog aktivnog centar u molekulima inhibitora. Adsorpcija se ponaša prema Temkinovoj adsorpcionoj izoterml. Dodavanjem  $I^-$ ,  $Br^-$  i  $SCN^-$  jona u rastvor koji sadrži organske derivate povećava se efikasnost inhibicije sistema.*

**Ključne reči:** organski derivati; Inhibicija; ciklični stres; kisela sredina; nerđajući čelik 316L SS

*Originalni naučni rad*

*Primljeno za publikovanje: 17. 07. 2014.*

*Prihvaćeno za publikovanje: 14. 09. 2014.*